Article

pubs.acs.org/Biomac

Combined Analysis of Polycation/ODN Polyplexes by Analytical Ultracentrifugation and Dynamic Light Scattering Reveals their Size, Refractive Index Increment, Stoichiometry, Porosity, and Molecular Weight

Yves Niebel, Michael D. Buschmann, Marc Lavertu,*[,‡] and Gregory De Crescenzo*[,‡]

Department of Chemical Engineering, Groupe de Recherche en Sciences et Technologies Biomédicales, École Polytechnique de Montréal, P.O. Box 6079, succ. Centre-Ville, Montréal Quebec, Canada H3C 3A7

Supporting Information

ABSTRACT: Analytical ultracentrifugation (AUC) and dynamic light scattering (DLS) were combined to characterize polyplexes formed with 10 kDa chitosan or 10 kDa PEI and oligodeoxynucleotides (ODN). Combined analysis revealed that both polyplexes were highly porous (over 80%) and that their weight average hydrodynamic diameters were of 46 and 55 nm for chitosan/ODN and PEI/ODN complexes, respectively. Transformation of the sedimentation coefficient distribution to a size and molecular weight distribution gave an average molecular weight of 19 and 29 MDa for chitosan and PEI polyplexes, respectively. Data from AUC also allowed for the calculation of the actual d*n*/d*c* and N/P ratios of each polyplex. Additional data from scanning electron microscopy and static light scattering confirmed the conclusions that were initially derived from AUC and DLS, thus validating that the combination of AUC and DLS is a powerful approach to characterize polyplexes in terms of refractive index increment, size, and molecular weight distributions, as well as porosity.

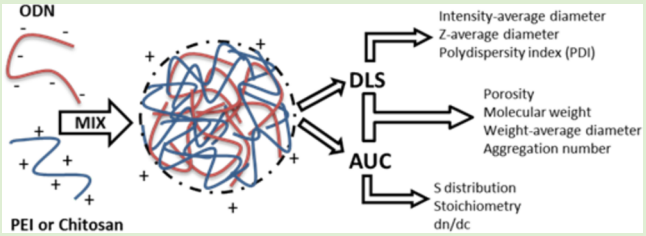

INTRODUCTION

Interest in the field of nonviral gene therapy has risen significantly in the past years due to some recent success in human clinical studies[1−3] of small interfering RNA (siRNA). As a result, a great diversity of siRNA delivery systems are currently being developed, including lipid nanoparticles (lipoplexes),[4] polymeric nanoparticles (polyplexes),[5,6] and siRNA conjugates.[7] Among cationic polymers, the synthetic polycation polyethyleneimine (PEI) is the most widely used to deliver siRNA,[8] while chitosan-derived vectors have garnered increasing interest as chitosan is biocompatible,[9] biodegradable,[10] and nontoxic.[11]

In order to establish clear structure−activity relationships for optimizing polyplexes, a complete characterization of their physicochemical properties relying on the use of multiple independent analytical techniques is required. Particle size and size distribution are the most widely assessed properties of these nanosized systems since they significantly influence their behavior and functionality. Among other important physicochemical properties are the surface charge, the molecular weight, and the amount of free excess polycation; the latter was recently shown to play a very determinant role in transfection.[12,13] Dynamic light scattering (DLS) and electron microscopy (EM) are commonly used techniques for size measurement,[14,15] while Doppler velocimetry and static light scattering (SLS) are used for ζ potential (surface charge) and molecular weight determination, respectively. A combined technique where asymmetrical flow-field flow fractionation (AF4) is coupled to light scattering and UV/vis spectroscopy was used recently to determine the size distribution and stoichiometry of chitosan-based polyplexes.[16]

Analytical ultracentrifugation (AUC) has become a powerful technique to characterize proteins and their interactions, since the development of new computer-based modeling relying on the Lamm equation.[17,18] It has also been proven to be of great interest for colloid analysis.[19,20] However, to the best of our knowledge, there is only one study in the literature reporting the use of AUC for the characterization of polycation/nucleic acid complexes.[21] As for AF4, AUC has the ability to separate species according to their size and, therefore, allows for the quantification of free excess polycations in polyplex solutions. Moreover, the sedimentation coefficient distribution provided by AUC can be converted into a hydrodynamic size distribution if one knows the particle partial specific volume while assuming that the particle is a compact sphere.[20] Such an assumption provides a minimal value of the hydrodynamic size and is appropriate for compact structures such as dense nanoparticle and globular proteins.[22] Although polyelectrolyte complexes such as polyplexes are much more compact than their individual constituents, the particle density (i.e., particle mass

Received: December 10, 2013
Revised: February 14, 2014
Published: February 26, 2014

divided by particle hydrodynamic volume) normally ranges from 0.3 to 0.7 g/mL and can even be lower, especially if the mismatching of the intercharge distance between the constituents is large.[23] A comparison of these values with the inverse of the partial specific volume of the polyplex constituents (e.g., 1.79 and 1.72 g/mL for DNA[24] and chitosan,[25] respectively) strongly suggests that these polyplexes are highly porous. Porosity values as high as 95% have been reported for chitosan−plasmid DNA complexes.[26,27] Their porosity must be known in order to precisely convert particle sedimentation coefficient into hydrodynamic size.

We report here a new approach for the characterization of polycation/nucleic acid complexes, which relies on a combination of AUC and DLS measurements in order to overcome the challenge associated with the inherent porosity of this type of nanoparticle. Polyplexes formed between siRNA-mimicking oligodeoxynucleotide (ODN) and chitosan or PEI were used as models to demonstrate the advantages of AUC/DLS combination to determine porosity, particle size, size distribution, molecular weight, stoichiometry, and incremental refractive index of polyplexes. For validation purposes, polyplexes were also characterized by SLS and EM.

THEORETICAL ASPECT

Sedimentation of a Porous Particle in a Centrifugal Field. The porous sphere model is used to represent the polyplex, and a nondraining behavior is assumed, a common assumption for polymers.[28] When placed in a centrifugal gravitational field, three forces are acting on the particle, namely the gravitational force $\vec{F}_s$ (eq 1), the buoyant force $\vec{F}_b$ (eq 2), and the frictional force $\vec{F}_f$ (eq 3), as previously reported:[29,30]

$$F_s = (1 - \varepsilon_p)\frac{4\pi}{3\bar{\nu}}a^3 \cdot \omega^2 r \tag{1}$$

$$F_b = -(1 - \varepsilon_p)\frac{4}{3}\pi a^3 \cdot \rho \cdot \omega^2 r \tag{2}$$

$$F_f = -f \cdot u = -f \cdot s \cdot \omega^2 r \tag{3}$$

where ω is the angular speed, r is the distance from the center of rotation, a, $\bar{\nu}$, and ε_p are the radius, the partial specific volume, and the porosity of the particle, respectively, ρ and η_s are the solvent density and viscosity, respectively, and u is the velocity of the particle when the three forces come into balance. It is noteworthy that the mass and the buoyant mass of the particle are corrected by the porosity parameter, ε_p, while the same frictional force as for a compact and nonporous sphere of equivalent size is considered to act on the polyplex since nondraining behavior is expected. The porosity is considered to be independent of the particle size, and the spheres were considered to be homogeneous throughout all calculations in this study. Using the Stokes−Einstein equation,[20] the diameter d_p can be deduced from the sedimentation coefficient using:

$$d_p = 2a = \sqrt{\frac{18 \cdot \eta \cdot s}{(1 - \varepsilon_p)(1/\bar{\nu} - \rho)}} \tag{4}$$

***c*(*s*) and *ls* − *g**(*s*) Models for the Analysis of AUC Sedimentation Profiles.** Two models were used here to analyze sedimentation data in this study. The $c(s)$ distribution model is based on the numerical resolution of the Lamm equation (eq 5) for ideal species that do not interact with each other. It is implemented into the SEDFIT software with a maximum entropy regularization.[18]

$$\frac{\partial c}{\partial t} = D\left(\frac{\partial^2 c}{\partial r^2} + \frac{1}{r}\frac{\partial c}{\partial r}\right) - \omega^2 s\left(r\frac{\partial c}{\partial r} + 2c\right) \tag{5}$$

where c is the mass concentration of a given species, ω is the angular speed, D is the diffusion coefficient, s is the sedimentation coefficient, t is the time, and r is the radius or distance from the center of rotation. This model was used for the analysis of the sedimentation data of single species.

The least-squares boundary model, known as the $ls - g^*(s)$ distribution, is also based on the numerical resolution of the Lamm equation (eq 5), but for ideal noninteracting and nondiffusing species ($D = 0$). It is also also implemented in the SEDFIT software, but with a Tikhonov−Philips regularization procedure.[31] This model was used for the analysis of the sedimentation data of polyplexes.

The weight-average diameter of polyplexes was determined from the sedimentation coefficient distribution as follows:

$$d_{p,w,AUC} = \frac{\int ls - g^*(s) \cdot d_p(s) \cdot ds}{\int ls - g^*(s) \cdot ds} \tag{6}$$

where $d_p(s)$ is the diameter calculated with eq 4.

Intensity-Weighted Average Hydrodynamic Diameter Derived from AUC. The intensity-weighted average hydrodynamic diameter (also provided by DLS), $d_{p,I,AUC}$, was also calculated from the $ls - g^*(s)$ distribution as follows:

$$d_{p,I,AUC} = \frac{\int ls - g^*(s) \cdot d_p(s)^4 \cdot ds}{\int ls - g^*(s) \cdot d_p(s)^3 \cdot ds} \tag{7}$$

This calculation of $d_{p,I,AUC}$ (for comparison with DLS results) assumes Rayleigh scattering, i.e. an isotropic scattering with intensity that is proportional to the square of the particle mass or, equivalently, to the sixth power of its size (R^6). The DLS size distributions of polyplex (Figures S6 and S8 in Supporting Information [SI]) revealed that most of the particles were sufficiently small to be considered as Rayleigh scatterers (for an angle of detection of 173° and a laser wavelength of 633 nm, the R^6 dependence of intensity was satisfied for hydrodynamic diameters up to about 100 nm or so), and the use of eq 7 was thus appropriate.

Calculation of Porosity by Combining AUC and DLS. The porosity, ε_p, was calculated from the intensity-weighted average diameters measured by DLS, $d_{p,I,DLS}$, and determined by AUC, $d_{p,I,AUC}$, supposing that particles were not porous ($\varepsilon_p = 0$). Considering that DLS and AUC intensity-weighted diameters should be equal, the porosity parameter was calculated by combining eqs 4 and 7:

$$\varepsilon_p = 1 - \left(\frac{d_{p,I,AUC}(\varepsilon_p = 0)}{d_{p,I,DLS}}\right)^2 \tag{8}$$

Note that mixing ODN and polycation (PEI or Chitosan) may have created polyplexes being polydisperse in terms of their porosity. This type of polydispersity cannot be taken into account by our model. It is reasonable to assume that the use of an average value for this parameter does not significantly affect the conclusions of the analysis. More precisely, if the polydispersity related to porosity is size-independent, the use of an average value is adequate.

Number-Weighted Average Diameter and Weight-Average Molecular Weight Derived from AUC. Number-weighted average diameter, $d_{p,N,AUC}$, was calculated from the $ls - g^*(s)$ distribution by including the porosity derived from eq 8 as follows:

$$d_{p,N,AUC} = \frac{\int \frac{ls - g^*(s)}{d_p^3(s)} \cdot d_p(s) \cdot ds}{\int \frac{ls - g^*(s)}{d_p^3(s)} \cdot ds} \quad (9)$$

Number-weighted average diameter was determined for comparison with SEM results.

Similarly, weight average molecular weight, $M_{w,AUC}$, was calculated from the $ls - g^*(s)$ distribution by correcting the mass of compact sphere with the porosity derived from eq 8 as follows:

$$M_{w,AUC} = \frac{\int ls - g^*(s) \cdot (1 - \varepsilon_p) \frac{4\pi}{3\bar{v}} \left(\frac{d_p(s)}{2}\right)^3 \cdot ds}{\int ls - g^*(s) \cdot ds} \quad (10)$$

$M_{w,AUC}$ was calculated for comparison with results from SLS.

MATERIALS AND METHODS

Materials. Ultrapure chitosan with a degree of deacetylation (DDA) of 92.7% was depolymerized using nitrous acid to achieve a number-weighted average molecular weight (M_n) of 10 kDa following a previously published procedure.[15] Molecular weight distribution and DDA were determined by size exclusion chromatography[32] and ^{1}H NMR,[33] respectively. Briefly, chitosan number- and weight-average molecular weights were determined by gel permeation chromatography coupled with a multiangle laser light scattering detector (Wyatt Technology Co, Santa Barbara, CA) and two Shodex OHpak (SB-806 M HQ and SB-805 HQ; Showa Denko America, Inc., New York, NY) columns eluted with a pH 4.5 acetic acid (0.15 M)/sodium acetate (0.1 M)/sodium azide (0.4 mM) buffer, as previously described.[32] Oligodeoxynucleotide: sense 5′-GTCATCACACTGAATACCAAT-3′; antisense: 5′-ATTG-GTATTCAGTGTGATGACAC-3′ (M_w 13451.9 Da), which is an ApoB1 siRNA-mimicking[34] ODN, was from IDT. Briefly, the two complementary single-stranded oligonucleotides were synthesized, then mixed at an equimolar ratio, annealed by heating at 95 °C for 5 min and slowly cooling to room temperature before drying, by the supplier. Linear polyethylenimine (product no.: 765090) and hydrochloric acid (1 N) were from Sigma. Chitosan and PEI properties are shown in Table 1.

Table 1. Molecular Characteristics of Chitosan and PEI

	M_n (kDa)	polydispersity index (PDI)	DDA (%)
chitosan	8.1	1.2	92.7
PEI	9.7[a]	1.2[a]	–

[a]Values from the supplier.

Preparation of the ODN/Polycation Complexes. Chitosan (5 mg/mL) and PEI (2 mg/mL) stock solutions were prepared by dissolving the polymer overnight in deionized water and HCl with HCl:glucosamine or HCl:ethyleneimine molar ratios of 1. ODN was dissolved in deionized water. All polymer stock solutions were filtered through a 0.2 μm filter prior to use. Complexes were formed by adding an equal volume (between 50 and 500 μL) of polycation solution into a 100 μg/mL ODN solution. Mixing was done by quickly pipetting up and down the final solution. Samples were allowed to incubate at room temperature for 30 min before DLS, SLS, and EM analysis. For AUC experiments, samples were placed directly into the instrument to reach thermal equilibrium. All polyplexes were prepared at an amine:phosphate molar ratio (N/P ratio) of 5, i.e., for a 100 μg/mL ODN solution, a 270 μg/mL chitosan solution or a 65 μg/mL PEI solution was used to prepare polyplexes. All experiments were performed in the presence of 10 mM NaCl, the concentration that was determined to be necessary to eliminate any electrostatic contributions to the sedimentation coefficient. This final ionic strength was achieved by adding a volume of 50 mM NaCl solution corresponding to 20% of the sample volume, a few minutes after polyplex preparation. For dn/dc measurement and the determination of the N/P ratios of the PEI/ODN polyplexes, the complexes were prepared using a 200 μg/mL ODN solution. The concentration of polycation solution was adjusted accordingly in order to maintain a mixing N/P ratio of 5.

Analytical Ultracentrifugation. AUC of all polyplex samples was performed using a ProteomeLab XL-I instrument (Beckman Coulter) equipped with a titanium eight-hole rotor (Beckman Coulter, An-50 Ti). The cells were assembled with sapphire windows and Epon charcoal-filled double sector, 12 mm path length centerpieces. The reference and the sample sectors were filled with 400 μL of 10 mM NaCl aqueous solution and 400 μL of sample solution, respectively. All the experiments were performed at 20 °C, and the samples were placed in the centrifuge for at least one hour prior to centrifugation to ensure thermal equilibrium was reached for the analysis. For single species (ODN, PEI, chitosan), AUC speed was fixed at 50000 rpm (RCF = 200000g). Sedimentation profiles were collected by interference optics using a laser diode at 655 nm and analyzed using the $c(s)$ distribution. For polyplexes, the speed was fixed at 10000 rpm (RCF = 7300g). Sedimentation profiles were collected by measuring absorbance (260 nm) for polyplexes (following ODN) and analyzed using the $ls - g^*(s)$ distribution.

For each species, the partial specific volume reported in the literature was used, namely 0.56 mL/g for ODN,[24] 0.58 mL/g for chitosan,[25] 0.669 mL/g for PEI,[21] 0.58 mL/g for chitosan/ODN complexes,[26,27] and 0.50 mL/g for PEI/ODN complexes. We here assumed that the partial specific volumes of polymers/pDNA[21,33,34] and polymers/ODN complexes do not significantly differ. SEDNTERP software was used to determine the density and the viscosity of the 10 mM NaCl aqueous solution used as solvent.[35]

Refractive Index Increment and N/P Ratio Determination by AUC. *Refractive Index Increment of Single Species.* Chitosan, PEI, and ODN were diluted from stock solutions to achieve a final concentration of 0.5 g/L. Each solution was analyzed by AUC as described above at 50000 rpm using interference optics. The dn/dc of each species was calculated using the following equation:

$$\Delta J = \frac{l \cdot (dn/dc)}{\lambda} \cdot c \quad (11)$$

where ΔJ is the number of fringes calculated from the integration of the $c(s)$ distribution obtained with SEDFIT, l is the optical path, λ is the laser wavelength and c is the concentration of species.

Quantification of Unbound Polymers by AUC and Determination of the N/P Ratio of the Polyplexes. Concentration of excess free polycation in polyplex samples was determined by AUC at 50000 rpm using interference optics. After a few minutes, polyplexes had completely sedimented, and a new sedimentation boundary corresponding to the lower mass species appeared. It is noteworthy that the absorbance at 260 nm revealed no free ODN left in the solution after complete sedimentation of the polyplexes. Concentration of the free polymer was determined by integrating the $c(s)$ distribution peak corresponding to the polymers species and using the dn/dc of the polymer previously calculated using eq 11. The polyplex N/P ratio was then calculated by using the following equation:

$$N/P_{\text{polyplex}} = \frac{(c_{\text{p,t}} - c_{\text{p,f}})\cdot N_{\text{N}}}{c_{\text{ODN}}\cdot N_{\text{P}}} \tag{12}$$

where $c_{\text{p,t}}$ is the total mass concentration of polymers, $c_{\text{p,f}}$ is the mass concentration of free polymers after mixing, c_{ODN} is the concentration of ODN, N_{N} is the number of amine groups per mass unit of polymers and N_{P} is the number of phosphate groups per mass unit of ODN.

Note that, as mentioned for porosity, the calculated N/P ratio is an average value that does not entirely describe the potential polydispersity of the N/P ratio for the resulting polyplexes.

Refractive Index Increment of Polyplexes. The dn/dc of polyplexes was determined at 10000 rpm using eq 11. The mass concentration of polyplexes was calculated from the known concentration of ODN and polymer as well as from the N/P ratios of the mix and of the resulting polyplexes using:

$$c_{\text{polyplex}} = c_{\text{ODN}} + \frac{c_{\text{polymer}}\cdot N/P_{\text{polyplex}}}{N/P_{\text{mix}}} \tag{13}$$

where c_{polyplex} is the mass concentration of polyplexes, c_{ODN} is the mass concentration of ODN, c_{polymer} is the total mass concentration of polymer, N/P_{polyplex} is the polyplex stoichiometry (eq 12), and N/P_{mix} is the mixing N/P ratio.

Determination of the Number of ODN and Polymer Per Particle. The weight-average number of ODN and polymer molecules per particle were determined from the calculated weight-average molecular weight (eq 10) and the polyplex N/P ratio (N/P_{polyplex}, eq 12) as follows:

$$N_{\text{ODN}} = M_{\text{w,AUC}}\left(\text{MW}_{\text{ODN}} + \frac{q_{\text{ODN}}\cdot N/P_{\text{polyplexes}}}{q_{\text{polycation}}}\text{MW}_{\text{polycation}}\right)$$

$$N_{\text{polycation}} = N_{\text{ODN}}\left(\frac{q_{\text{ODN}}\cdot N/P_{\text{polyplexes}}}{q_{\text{polycation}}}\right) \tag{14}$$

where N_{ODN} and $N_{\text{polycation}}$ are the number of ODN and polycation molecules within the particle, respectively, $M_{\text{w,AUC}}$ is the weight-average molecular weight of polyplex calculated using eq 10, MW_{ODN} and $\text{MW}_{\text{polycation}}$ are the molecular weight of ODN and polycation molecules (number-weighted average molecular weight, Table 1), respectively, and q_{ODN} and $q_{\text{polycation}}$ are the number of charges or ionizable moieties per molecule of ODN and polycation, respectively. Here, chitosan, PEI, and ODN, bear 46, 220, and 44 charges or ionizable moieties per molecule on average, respectively.

Dynamic Light Scattering and Static Light Scattering. DLS and SLS were performed at 20 °C on a Zetasizer Nano ZS (Malvern Instrument) with a laser wavelength of 633 nm and a scattering detection of 173°. SLS was performed for samples diluted to 5, 7.5, 10, 12.5, 15, 17.5, and 20 μg/mL of ODN. For each concentration, one DLS measurement with one read-out, using both the CONTIN algorithm and the cumulant fit was also performed. Toluene was used as reference solution for SLS measurements. Solutions were analyzed from the lowest to the highest concentration in order to obtain a Debye plot by applying the Rayleigh equation (eq 15), from which the weight average molecular weight of the polyplexes, M_{w}, is determined by an extrapolation to infinite dilution:

$$\frac{Kc}{R_\theta} = \left(\frac{1}{M_{\text{w}}} + 2A_2c\right)P(\theta) \tag{15}$$

where A_2 is the second virial coefficient, R_θ is the Rayleigh ratio, i.e. the ratio of scattered light to incident light for $\theta = 173°$, c is the polyplex mass concentration calculated from the polyplex N/P ratio (eq 13), $P(\theta)$ the angular dependence of the polyplex scattering intensity, and K is an optical constant given by:

$$K = \frac{2\pi}{\lambda_0{}^4 N_{\text{A}}}(n_0(\text{d}n/\text{d}c))^2 \tag{16}$$

where λ_0 is the laser wavelength, N_{A} is the Avogadro's constant, n_0 is the solvent refractive index, and dn/dc is the refractive index increment of the polyplexes measured by analytical ultracentrifugation as described above.

A spherical shape correction implemented in the manufacturer software was applied, in agreement with the spherical morphology revealed by EM (see Figure 2).

Scanning Electron Microscopy. Samples were prepared using a Badger 250 mini spray to pulverize the polyplex solutions on a silicon substrate, which was subsequently coated with gold. SEM analysis was performed using an environmental SEM (ESEM, Quanta 200 FEG, FEI Company Hillsboro, OR). The high vacuum mode of the ESEM microscope was employed for greater resolution and increased contrast. An accelerating voltage of 20 kV, a spot size of 3, and a working distance of 5 mm were used. For each sample, five to six images were acquired and 10 particles/image were characterized for their size. Mean size and standard deviation were calculated from these 50−60 measurements.

Statistics. Mean and standard deviation for each result were calculated from three independent experiments ($N = 3$) for AUC, SLS, and DLS experiment.

RESULTS AND DISCUSSION

Separation of Free Polymer and Polyplex by AUC Allows for the Precise Determination of Polyplex Refractive Index Increment and Stoichiometry. The determination of the refractive index increment (dn/dc) of all single species and polyplexes was essential to calculate the N/P ratio as well as to measure the molecular weight of polyplexes by SLS. dn/dc values of 0.189, 0.293, and 0.168 mL/g were found for chitosan, PEI and ODN, respectively (Table 2). Refractive index increment determined by AUC for chitosan and ODN are in good agreement with previously reported values (Table 2). The slight discrepancy found for PEI (namely 0.293 mL/g in this study vs 0.263−0.272 mL/g in the literature[36] is most likely due to differences between the solvent used in the different studies (10 mM NaCl solution in this study versus 1% formic acid[36]).

Table 2. Refractive Index Increment d*n*/d*c* of the Different Species

	d*n*/d*c* measured by AUC (mL/g)	d*n*/d*c* from the literature (mL/g)
chitosan	0.189 ± 0.002	0.190–0.192[32,37]
PEI	0.293 ± 0.004	0.263–0.272[36]
ODN	0.168 ± 0.002	0.168–0.171[14,38]
chitosan/ODN polyplexes	0.117 ± 0.005	n.a.
PEI/ODN polyplexes	0.152 ± 0.001	n.a.

We also determined the concentration of free polymer by analyzing the sedimentation profile of the remaining polymer at high speed (Table 3), as previously reported.[21] These values of

Table 3. Concentration of Free Polymers and Polyplex N/P Ratios (calculated with eq 12)

			N/P ratio	
polyplexes	$c_{p,t}$ (μg/mL)	$c_{p,f}$ (μg/mL)	AUC results	literature
chitosan/ODN	108	79 ± 2	1.3 ± 0.1	1.2–1.6[16]
PEI/ODN	52	25 ± 1	2.4 ± 0.1	2.4–2.5[21,39]

free polymer concentration allowed us to calculate the N/P ratios of the chitosan/ODN and PEI/ODN complexes of 1.3 and 2.4, respectively (Table 3). These N/P ratios are in agreement with those determined using AF4 or Orange II titration (for chitosan) as well as with AUC or a copper-based colorimetric approach (for PEI) (Table 3). Using these polyplex N/P ratios, d*n*/d*c* values of 0.117 mL/g and 0.152 mL/g were then deduced for chitosan/ODN and PEI/ODN polyplexes, respectively, from eqs 11 and 13 (Table 2).

In our study, the d*n*/d*c* of polyplexes was directly measured by AUC instead of being calculated by relying on the common assumption of the additivity of the refractive index increment of the two components,[14] namely the polycation and the ODN. Furthermore, our results strongly suggest that the additivity of the refractive index increment of the two components is not applicable to highly interacting multicomponent systems, such as polyplexes. Indeed, the additivity assumption would have given theoretical values ranging between the d*n*/d*c* values of singles species, whereas our experimental protocol gave values below this range (Table 2). Thus, AUC stands out as a technique of choice in order to measure d*n*/d*c* for polyplexes since, in contrast to standard refractometry measurements, AUC has the ability to separate complexes from free species. It is noteworthy to recall that the d*n*/d*c* values required for SLS measurements are those corresponding to complexes, the scattering of the free polymer being negligible when compared to that of the complexes.

Combining AUC and DLS Allows for the Calculation of Porosity, Size Distribution, Aggregation Number, and Molecular Weight of Polyplexes. AUC profiles corresponding to three independent preparations of each type of polyplex (Figure 1A) demonstrated that our experimental protocol was reproducible with manual mixing of ODN and polycations. Furthermore, no sign of polyplex aggregates was present in our samples, in stark contrast with PEI/plasmid DNA polyplexes studied by Perevyazko and colleagues.[21] Analysis of the $ls-g^*(s)$ distribution gave a weight average sedimentation coefficients, S_w, of 100 and 299 S for chitosan/ODN and PEI/ODN polyplexes, respectively, which are at least 20×

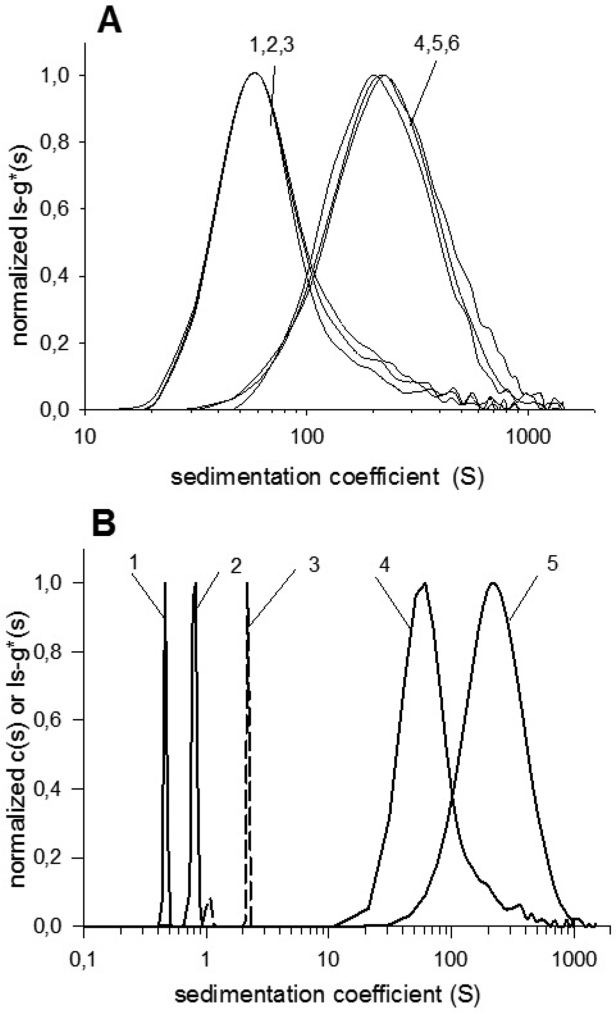

Figure 1. (A) Reproducibility of (1–3) chitosan/ODN and (4–6) PEI/ODN polyplexes as investigated by AUC. (B) Sedimentation coefficient distribution of (1) PEI, (2) Chitosan, (3) ODN, (4) Chitosan/ODN and (5) PEI/ODN polyplexes. Sedimentation was performed at 50,000 and 10,000 rpm for single species and polyplexes, respectively.

higher than those of the individual constituent species (Figure 1B).

A preliminary interpretation of these AUC data, assuming that the polyplexes are compact and spherical, gave intensity-weighted average diameters of 31 and 34 nm for chitosan/ODN and PEI/ODN complexes (as calculated using eq 6). These values were directly compared to the intensity-weighted average diameter of the same polyplexes, determined by DLS where diameters of 97 and 82 nm were found for the chitosan/ODN and PEI/ODN polyplexes, respectively (Table 4). The lower sizes from AUC did not account for the highly porous nature of our polyplexes. The porosity (ε_p) could then be calculated by combining AUC and DLS intensity-weighted average diameters using eq 8. ε_p was thereby calculated to be 90% and 83% for chitosan/ODN and PEI/ODN complexes, respectively. Introducing the porosity in eq 4, the weight-average diameters for chitosan/ODN and PEI/ODN polyplexes were found to be 46 and 55 nm, respectively (Table 6), as calculated by eq 6.

Porosity was previously introduced theoretically for charged porous spherical nanoparticles exposed to a constant gravita-

dx.doi.org/10.1021/bm4018148 | Biomacromolecules 2014, 15, 940–947

Table 4. Estimation of Porosity ε_p Based on the AUC and DLS Results and Eq 8 for Both Polyplexes

polyplexes	S_w (S)	$d_{p,I,AUC}$ [a] (nm)	$d_{p,I,DLS}$ (nm)	$d_{z-average,DLS}$ (nm)	PDI	ε_p
chitosan/ODN	100 ± 7	31 ± 1	97 ± 7	72 ± 4	0.23 ± 0.02	90% ± 1% [b]
PEI/ODN	299 ± 10	34 ± 6	82 ± 5	68 ± 4	0.18 ± 0.02	83% ± 4% [b]

[a]Assuming that the polyplexes are nonporous. [b]Standard deviation calculated from three independent experiments.

tional field in other studies.[29,30] In this study we assumed a nondraining situation in which the fluid within the particle moves along with it. To the best of our knowledge, porosity corrections were never applied to sedimentation velocity experiments and never combined with DLS in order to characterize polyplexes. Porosity values we calculated in the case of chitosan/ODN polyplexes are close to the value found in the literature for scaffolds made of chitosan and plasmid DNA.[26,27] The calculation of porosity implied the use of intensity-weighted average diameters derived from both DLS and AUC (see eq 8). For AUC data, the calculation of the intensity−weighted average diameters assumes Rayleigh-type scatterers (i.e., particles with scattered intensities proportional to the sixth power of the radius). Such an approximation held true for most of the particles corresponding to each type of polyplex under study, as revealed by SEM (Figure 2). PEI-derived polyplexes were found to be less porous than their chitosan counterparts, more likely due to higher mismatch of intercharge spacing between chitosan and ODN when compared to that of PEI and ODN (0.52 nm for chitosan,[40] 0.25−0.35 nm for PEI[41] and 0.17 nm[40] for ODN). Indeed, intercharge spacing mismatches are known to induce swelling of polyelectrolyte complexes.[23]

Pioneering work of Pereviazko et al.[21] studied PEI/pDNA polyplexes by AUC;[21] however, the authors did not introduce porosity in their analysis of AUC results. Sedimentation coefficients reported by Pereviazko et al.[21] were significantly higher than the ones we report here (10000 vs 300 S). This difference is most likely due to the presence of aggregates since PEI/DNA polyplexes are prone to aggregation at physiological pH and high salt concentrations (as used in their study). In contrast, we used only 10 mM salt concentration and acidic conditions to ensure colloidal stability of polyplexes.

Having determined the N/P ratio and the weight average molecular weight for each particle, by AUC, it is possible to determine the aggregation number (i.e., the number of copies of each species within a single polyplex—see Table 5). Interestingly, both polyplex types are characterized by amounts of ODN being within the same order of magnitude, despite the significant physicochemical differences between polycations.

SEM Imaging Confirms the Spherical Shape of Both Polyplexes and Their Size, As Determined by DLS/AUC. Further investigations of our polyplexes by SEM unambiguously confirmed the spherical shape of our polyplexes (Figure 2A−D). Diameters measured by SEM for both chitosan/ODN and PEI/ODN polyplexes were of 57 ± 13 and 45 ± 12 nm, respectively (Table 6, Figure 2 E,F), in agreement with number-weighted average diameter values (eq 9) derived from AUC experiments (40 and 46 nm for chitosan/ODN and PEI/ODN polyplexes, respectively).

SLS Weight-Average Molecular Weight Measurement Supports Conclusions from AUC/DLS about Porosity. Weight-average molecular weights of 20 and 14 MDa (Table 7) were derived from SLS Debye plots (using eqs 15 and 16) of chitosan/ODN and PEI/ODN polyplexes, respectively. Given our measured polyplex porosity (Table 4), one can transform the $ls - g^*(s)$ distribution (Figure 1) into a molar mass distribution, and thus calculate the weight average molecular

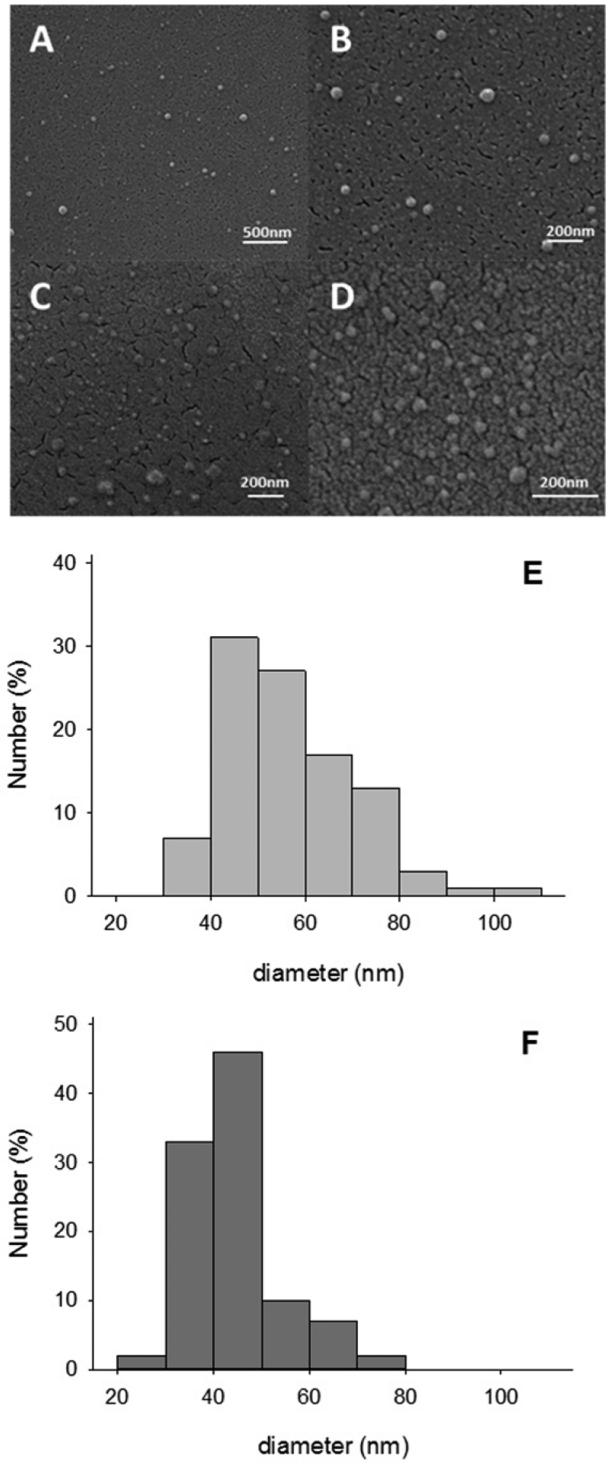

Figure 2. SEM images of (A, B) chitosan/ODN and (C, D) PEI/ODN polyplexes. Polyplex size distribution from SEM imaging for (E) chitosan/ODN and (F) PEI/ODN polyplexes.

Table 5. Aggregation Number Related to Both Polyplexes

polyplexes	$M_{w,AUC}$(kDa)	number of ODN	number of polycations
chitosan/ODN	19000 ± 3000	780 ± 120	1000 ± 160
PEI/ODN	29000 ± 4000	1580 ± 220	790 ± 110

Table 6. Number-Weighted Average Diameter Calculated from SEM Imaging and AUC and Weight Average Diameter Calculated from AUC

polyplexes	$d_{p,N,SEM}$ (nm)	$d_{p,N,AUC}$ (nm)	$d_{p,w,AUC}$ (nm)
chitosan/ODN	57 ± 14[a]	40 ± 1[c]	46 ± 3[c]
PEI/ODN	45 ± 10[b]	46 ± 1[c]	55 ± 3[c]

[a]Standard deviation calculated from 100 measurements from six different pictures. [b]Standard deviation calculated from 60 measurements from five different pictures. [c]Standard deviation calculated from independent experiments (N = 3).

Table 7. M_w Deduced from SLS and AUC Measurements

polyplexes	$M_{w,SLS}$ (MDa)	$M_{w,AUC}$ (MDa)
chitosan/ODN	20 ± 1.4	19 ± 3
PEI/ODN	13.9 ± 0.6	29 ± 4

weight of the different polyplexes using eq 10. This gives a weight average molecular weight of 19 and 29 MDa for chitosan/ODN and PEI/ODN polyplexes, respectively (Table 7). While excellent agreement was found comparing weight-average molecular weights from AUC to SLS for chitosan-based polyplexes (Table 7), in the case of PEI-based polyplexes, the molecular weight measured by AUC was 2-fold higher than that measured by SLS. Such a discrepancy may arise from the precision of both AUC and SLS measurements. Furthermore, a closer inspection of the Debye plot of PEI/ODN samples (Figure S7 in SI) revealed a slightly negative second virial coefficient, which is indicative of attractive interactions that could induce aggregation and thus compromise the precision of the measurement (note that the second virial coefficient for chitosan-based polyplexes was positive, indicating repulsion between chitosan-based polyplexes). Nevertheless, molecular weights that were deduced from AUC and SLS measurements were within the same order of magnitude, thus strongly supporting once again the porous nature of our polyplexes.

CONCLUSION

We have demonstrated that a combination of AUC and DLS measurements constitutes a powerful approach for a detailed characterization of polycation/ODN polyplexes. Of salient interest, the use of AUC alone allowed for the determination of the N/P ratio (stoichiometry) and refractive index increment of the polyplexes. The latter cannot be predicted by additivity rules previously applied to noninteracting multicomponent systems. Accurate dn/dc data is crucial for precise molecular weight determination from SLS measurements. Moreover, a combination of AUC and DLS allowed for the determination of almost all physicochemical parameters of polyplexes under study, including sedimentation coefficient distribution, size distributions, molecular weight distributions, and porosity. Additional measurements performed by SLS and SEM validated the conclusions derived from AUC and DLS techniques.

ASSOCIATED CONTENT

Supporting Information

More experimental data as well as AUC, DLS and SLS results. This material is available free of charge via the Internet at http://pubs.acs.org.

AUTHOR INFORMATION

Corresponding Authors

*gregory.decrescenzo@polymtl.ca or
*marc.lavertu@polymtl.ca.

Author Contributions

‡M.L. and G.D.C. contributed equally to this work.

Notes

The authors declare no competing financial interest.

ACKNOWLEDGMENTS

This work was supported by the Natural Sciences and Engineering Council of Canada (NSERC) (Y.N., M.L., M.B.) and the Canada Research Chair Protein-enhanced Biomaterials (G.D.C.). Y.N. received fellowships from the GRSTB (FRQ-S) and the MEDITIS (NSERC) programs as well as a scholarship grant from ENSTA ParisTech. The authors thank Monica Iliescu Nelea for technical assistance with SEM experiments.

REFERENCES

(1) Zimmermann, T.; Karsten, V.; Harrop, J.; Chan, A.; Chiesa, J.; Peters, G.; Falzone, R.; Cehelsky, J.; Nochur, S.; Vaishnaw, A.; Gollob, J. *J. Card. Failure* **2013**, *19* (8), S66.

(2) Davis, M. E. *Mol. Pharmaceutics* **2009**, *6* (3), 659−668.

(3) Burnett, J. C.; Rossi, J. J.; Tiemann, K. *Biotechnol. J.* **2011**, *6* (9), 1130−1146.

(4) Cardoso, A.; Trabulo, S.; Moreira, J. N.; Duzgunes, N.; de Lima, M. C. P. Targeted Lipoplexes for siRNA Delivery. In *Methods in Enzymology Liposomes, Pt G*; Duzgunes, N., Ed.; Elsevier Academic Press Inc: San Diego, 2009; Vol. *465*, pp 267−287.

(5) Holzerny, P.; Ajdini, B.; Heusermann, W.; Bruno, K.; Schuleit, M.; Meinel, L.; Keller, M. *J. Controlled Release* **2012**, *157* (2), 297−304.

(6) Mao, S. R.; Neu, M.; Germershaus, O.; Merkel, O.; Sitterberg, J.; Bakowsky, U.; Kissel, T. *Bioconjugate Chem.* **2006**, *17* (5), 1209−1218.

(7) Kumari, A.; Kumar, V.; Yadav, S. K. *Expert Opin. Biol. Ther.* **2011**, *11* (10), 1327−1339.

(8) Nimesh, S. *Curr. Clin. Pharmacol.* **2012**, *7* (2), 121−130.

(9) Mi, F. L.; Tan, Y. C.; Liang, H. F.; Sung, H. W. *Biomaterials* **2002**, *23* (1), 181−191.

(10) Onishi, H.; Machida, Y. *Biomaterials* **1999**, *20* (2), 175−182.

(11) de Campos, A. M.; Diebold, Y.; Carvalho, E. L.; Sanchez, A.; Alonso, M. J. *Pharm. Res.* **2004**, *21* (5), 803−810.

(12) Thibault, M.; Astolfi, M.; Tran-Khanh, N.; Lavertu, M.; Darras, V.; Merzouki, A.; Buschmann, M. D. *Biomaterials* **2011**, *32* (20), 4639−4646.

(13) Yue, Y. A.; Jin, F.; Deng, R.; Cai, J. G.; Chen, Y. C.; Lin, M. C. M.; Kung, H. F.; Wu, C. *J. Controlled Release* **2011**, *155* (1), 67−76.

(14) Lai, E.; van Zanten, J. H. *Biophys. J.* **2001**, *80* (2), 864−873.

(15) Lavertu, M.; Methot, S.; Tran-Khanh, N.; Buschmann, M. D. *Biomaterials* **2006**, *27* (27), 4815−4824.

(16) Ma, P. L.; Buschmann, M. D.; Winnik, F. M. *Anal. Chem.* **2010**, *82* (23), 9636−9643.

(17) Schuck, P. *Anal. Biochem.* **2003**, *320* (1), 104−124.

(18) Schuck, P. *Biophys. J.* **2000**, *78* (3), 1606−1619.

(19) Planken, K. L.; Coelfen, H. *Nanoscale* **2010**, *2* (10), 1849−1869.

(20) Mächtle, W.; Börger, L. *Analytical ultracentrifugation of polymers and nanoparticles*; Springer: Berlin, New York, 2006.

(21) Perevyazko, I. Y.; Bauer, M.; Pavlov, G. M.; Hoeppener, S.; Schubert, S.; Fischer, D.; Schubert, U. S. *Langmuir* **2012**, *28* (46), 16167−16176.

(22) Wilson, K.; Walker, J. M. *Principles and Techniques of Biochemistry and Molecular Biology*; Cambridge University Press: Cambridge, UK, 2005.
(23) Thunemann, A. F.; Muller, M.; Dautzenberg, H.; Joanny, J. F. O.; Lowen, H., Polyelectrolyte complexes. In *Polyelectrolytes with Defined Molecular Architecture II*, Schmidt, M., Ed.; Springer-Verlag: Berlin, 2004; Vol. *166*, pp 113−171.
(24) Bonifacio, G. F.; Brown, T.; Conn, G. L.; Lane, A. N. *Biophys. J.* **1997**, *73* (3), 1532−1538.
(25) Errington, N.; Harding, S. E.; Varum, K. M.; Illum, L. *Int. J. Biol. Macromol.* **1993**, *15* (2), 113−117.
(26) Fukushima, T.; Hayakawa, T.; Kawaguchi, M.; Ogura, R.; Inoue, Y.; Morishita, K.; Miyazaki, K. *Dent. Mater. J.* **2005**, *24* (3), 414−421.
(27) Fukushima, T.; Hayakawa, T.; Okamura, K.; Takeda, S.; Inoue, Y.; Miyazaki, K.; Okahata, Y. *J. Biomed. Mater. Res., Part B* **2006**, *76B* (1), 121−129.
(28) Ottinger, H. C. *Rheol. Acta* **1996**, *35* (2), 134−138.
(29) Liu, Y. C.; Keh, H. J. *Colloids Surf., A* **1998**, *140* (1−3), 245−259.
(30) Keh, H. J.; Chen, W. C. *J. Colloid Interface Sci.* **2006**, *296* (2), 710−720.
(31) Schuck, P.; Rossmanith, P. *Biopolymers* **2000**, *54* (5), 328−341.
(32) Nguyen, S.; Hisiger, S.; Jolicoeur, M.; Winnik, F. M.; Buschmann, M. D. *Carbohydr. Polym.* **2009**, *75* (4), 636−645.
(33) Lavertu, M.; Xia, Z.; Serreqi, A. N.; Berrada, M.; Rodrigues, A.; Wang, D.; Buschmann, M. D.; Gupta, A. *J. Pharm. Biomed. Anal.* **2003**, *32* (6), 1149−1158.
(34) Zimmermann, T. S.; Lee, A. C. H.; Akinc, A.; Bramlage, B.; Bumcrot, D.; Fedoruk, M. N.; Harborth, J.; Heyes, J. A.; Jeffs, L. B.; John, M.; Judge, A. D.; Lam, K.; McClintock, K.; Nechev, L. V.; Palmer, L. R.; Racie, T.; Rohl, I.; Seiffert, S.; Shanmugam, S.; Sood, V.; Soutschek, J.; Toudjarska, I.; Wheat, A. J.; Yaworski, E.; Zedalis, W.; Koteliansky, V.; Manoharan, M.; Vornlocher, H. P.; MacLachlan, I. *Nature* **2006**, *441* (7089), 111−114.
(35) Lebowitz, J.; Lewis, M. S.; Schuck, P. *Protein Sci.* **2002**, *11* (9), 2067−2079.
(36) Tarcha, P. J.; Pelisek, J.; Merdan, T.; Waters, J.; Cheung, K.; von Gersdorff, K.; Culmsee, C.; Wagner, E. *Biomaterials* **2007**, *28* (25), 3731−3740.
(37) Rinaudo, M. *Prog. Polym. Sci.* **2006**, *31* (7), 603−632.
(38) Fishman, D. M.; Patterson, G. D. *Biopolymers* **1996**, *38* (4), 535−552.
(39) Boeckle, S.; von Gersdorff, K.; van der Piepen, S.; Culmsee, C.; Wagner, E.; Ogris, M. *J. Gene Med.* **2004**, *6* (10), 1102−1111.
(40) Ma, P. L.; Lavertu, M.; Winnik, F. M.; Buschmann, M. D. *Biomacromolecules* **2009**, *10* (6), 1490−1499.
(41) Richard, I.; Thibault, M.; De Crescenzo, G.; Buschmann, M. D.; Lavertu, M. *Biomacromolecules* **2013**, *14* (6), 1732−1740.